Chapter 8
Balancing of a 3-DOFs Parallel Manipulator

D. Cafolla, G. Carbone, and M. Ceccarelli

Abstract This chapter gives an overview on static and dynamic balancing. Basic approaches are discussed for achieving the design of mechanisms having a fully balanced behavior under different operation conditions. A formulation is proposed to address the effects of balancing on mass distributions and dynamic performance. The proposed formulation is applied for the dynamic balancing of a three DOFs (degrees-of-freedom) spatial parallel manipulator, namely CaPaMan 2bis (Cassino Parallel Manipulator 2bis). This parallel manipulator has three identical legs, where each leg is composed by a four-bar mechanism, an orthogonal revolute joint, and a spherical joint that is attached on the mobile platform. The proposed solution for achieving the balancing of CaPaMan 2bis is based on the use of counter-rotary counterweights. The obtained results are validated by simulations by using a general-purpose software for multi-body dynamics analysis.

Keywords Parametric • Design • Optimization • Parallel manipulator

8.1 Introduction

Inertia forces exist wherever parts having mass are accelerated [1]. A careful attention to inertia forces must be given, since the first design steps. In fact, each moving part must be designed to perform satisfactorily under all combinations of inertia, payloads, and externally acting forces. Inertia forces are also important, since any resulting external or shaking force becomes a disturbing force on the supporting frame and associated parts. In both cases varying forces acting on elastic bodies can produce serious, even destructive, vibrations of the parts or complete machine and adjacent structures and equipments, as outlined for example in [1, 2]. The presence of vibration and the accompanying noise can provide serious problems to other machines and to human operators as discussed for example in [3].

D. Cafolla (✉) • G. Carbone • M. Ceccarelli
LARM: laboratory of Robotics and Mechatronics, DICEM, University of Cassino and South Latium Cassino, Cassino, Italy
e-mail: cafolla@unicas.it; carbone@unicas.it; ceccarelli@unicas.it

D. Zhang, B. Wei (eds.), *Dynamic Balancing of Mechanisms and Synthesizing of Parallel Robots*, DOI 10.1007/978-3-319-17683-3_8

Several applications in many different fields can get significant advantages from balancing. Very well known is, for example, the balancing of rotors or tyres that has been even coded in international standards such as [4, 5]. In the robotic field the balancing of manipulators with large payloads is often considered for the static and/or dynamic balancing of industrial robots with high payloads, since it may significantly reduce the power consumption [6, 7]. Balancing is also important to reduce wear for machine tools or to improve the operation comfort (by reducing vibrations) such as reported for example in [8]. The operation comfort is a key issue in applications such as flight simulators [9] or in any application requiring human-robot interaction, such as the rehabilitation of patients as proposed in [10]. Careful attention to dynamic balancing is usually addressed, for example, when designing and operating single-wheel robots such as in [11] or biped and humanoid robots such as reported in [12].

A general approach for minimization of the magnitude of the inertial shaking forces can be formulated by introducing another shaking force that is equal in magnitude and opposite in direction to the original shaking force. This process is called balancing [1–6]. Based on this concept, several balancing techniques have been developed and they can be found in a very rich literature such as reported in [13–23]. Further investigations are still undergoing for identifying balancing techniques that can better fit to specific applications such as reported in [24–33] or for implementing specific optimal design procedures such as proposed by [34, 35].

In this chapter we propose a formulation to address the effects of balancing on mass distributions and dynamic performance. The proposed formulation can be seen as a tool for designers in selecting the most appropriate solution(s) according to the expected operation conditions. The proposed formulation can be conveniently applied for the balancing of parallel manipulators. A specific case of study has been developed by referring to a three-degrees-of-freedom (3-DOFs) spatial parallel manipulator by designing proper counter-rotary counterweights (CRCW).

8.2 Problems and Requirement for Balancing

8.2.1 Static Balancing

A mechanism is statically balanced if its potential energy is constant for all possible configurations. Static balance of a body occurs when the center of gravity of the object is laying on its axis of rotation and the object can remain stationary without the application of any force [1].

A simple example of static balancing can be made by referring to a disk as shown in the schemes of Fig. 8.1. In particular, Fig. 8.1a shows a disk having an irregular shape. Due to this shape the center of mass of the disk is not laying on the axis of rotation. The disk is not statically balanced and it has a tendency to rotate due to the

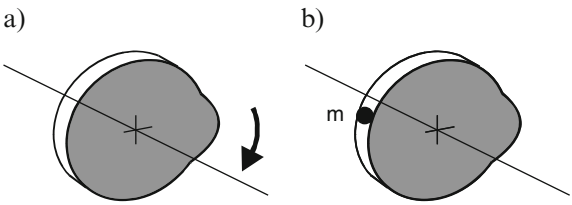

Fig. 8.1 Schemes of a disk: (**a**) The lack of static balancing lets the disk turn to the force of gravity; (**b**) a counterweight mass *m* is added to balance the disk

force of gravity. Static balancing is usually achieved by using additional mechanical elements like elastic components or counterweight masses, either directly mounted on the links of the mechanism or by using auxiliary components [1, 6, 7].

The static balancing of the disk in Fig. 8.1a can be easily achieved by using a counterweight mass m as shown in Fig. 8.1b. This counterweight mass will move the center of mass to let it coincide with the axis of rotation. Accordingly, the disk will no more have a tendency to rotate about its axis of rotation.

The calculation of the counterweight mass and location is made by considering the centrifugal force F_c of the disk in the form

$$F_c = M\,\omega^2\,r \tag{8.1}$$

where M is the mass of the disk, ω is the angular speed of rotation of the disk, and r is the radial distance of the center of mass from the rotation axis.

One can add a mass m at a radius r_m to the disk so that the resulting centrifugal force will become zero such as shown in the scheme of Fig. 8.1b. Accordingly one can write Eq. (8.1) in the forms

$$F_c = 0 = M\,\omega^2\,r - m\omega^2\,r_m \tag{8.2}$$

$$M\,\omega^2\,r = m\,\omega^2\,r_m \tag{8.3}$$

If the angular speed ω is nonzero, one can divide both sides of Eq. (8.3) by ω so that one can obtain the following expression of the required mass for letting the centrifugal force become zero as

$$m \;\; = M\;\; r/r_m \tag{8.4}$$

8.2.2 Dynamic Balancing

A rotating system of mass is in dynamic balance when the rotation does not produce any resultant centrifugal force or couple. Thus, the system rotates without requiring the application of any external force or couple, other than that required to support its weight [1]. Statically balanced disks such as in Fig. 8.1b may still be dynamically unbalanced due to the presence of centrifugal effects.

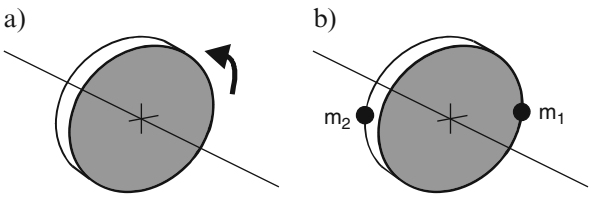

Fig. 8.2 Schemes of a disk: (**a**) The lack of dynamic balancing produces a couple acting on the rotating axis; (**b**) counterweight masses m_1 and m_2 are added to dynamically balance the disk

Dynamically unbalanced rotating shafts are usually balanced by adding two identical weights m_1 and m_2, as shown in the schemes of Fig. 8.2.

The two masses m_1 and m_2 will not modify the static balancing while they will produce a counterclockwise centrifugal effect that will achieve the dynamic balancing.

Several approaches can be used for dynamic balancing of mechanisms. The classical method to obtain statically and dynamically balanced mechanisms consists on adding mass and inertia elements to the system so that the center of mass remains unchanged (statically balanced) while the angular momentum becomes zero for any motion. The dynamic balancing can be achieved using several methods or "principles." For example, [19, 20] propose the following methods:

- Using counter-rotary counter-masses
- Using separate counter-rotations
- Using idler loops
- Using a duplicated mechanism

Similarly, [14, 15] propose the following methods:

- Balancing by counterweights mounted on the movable links
- Harmonic balancing by two counter-rotating masses
- Balancing by opposite movements

The balancing by counterweights is based on adding counterweight masses that can have the same weight and opposite dynamic effects of the links being part of the mechanism to be balanced. In the case of complete shaking force balancing this approach is generally limited to simple mechanisms having only revolute joints.

The harmonic balancing by two counter-rotating masses is based on harmonic analysis. The reduction of inertia effects is accomplished by the balancing only of certain harmonics of the shaking forces and shaking moments. Unbalanced forces and moments are approximated by Fourier series (or Gaussian least-square formulation) and then each frequency component is studied. This approach has been used successfully for engine balancing. For example, the balancing shafts are used for balancing of a second harmonic of the shaking force.

The balancing by opposite movements requires the addition of an axially symmetric duplicate mechanism that will produce opposite motions and dynamic effects as compared with the mechanism to be balanced. In this case, shaking force and shaking moment can become both zero.

The balancing by added dyads is achieved when adding links (dyads) to a mechanism to make a parallelogram chain (consisting of the initial links of the mechanism and the added dyad). In this way, the dyad transfers the motion of the coupler link to a shaft on the frame, where it is connected to a counterweight of considerably reduced mass as reported for example in [28]. In this way, it is possible to create an additional balancing moment for reducing the shaking moment while maintaining the static balance of the mechanism.

The major drawback of most of the abovementioned approaches is that a considerable amount of mass and inertia is added to the system, and: "The price paid for shaking force and shaking moment balancing is discouraging" [16]. Another possible approach is to generate trajectories which minimize or eliminate reaction forces and torques [32]. This approach is however quite restrictive and applicable only for special cases.

8.2.3 A Procedure for Balancing

In Fig. 8.3 a general procedure is outlined for solving a problem of balancing.

The first step of the procedure is the definition of proper kinematic and dynamic. It is to note that identifying general formulations for the solution of kinematic

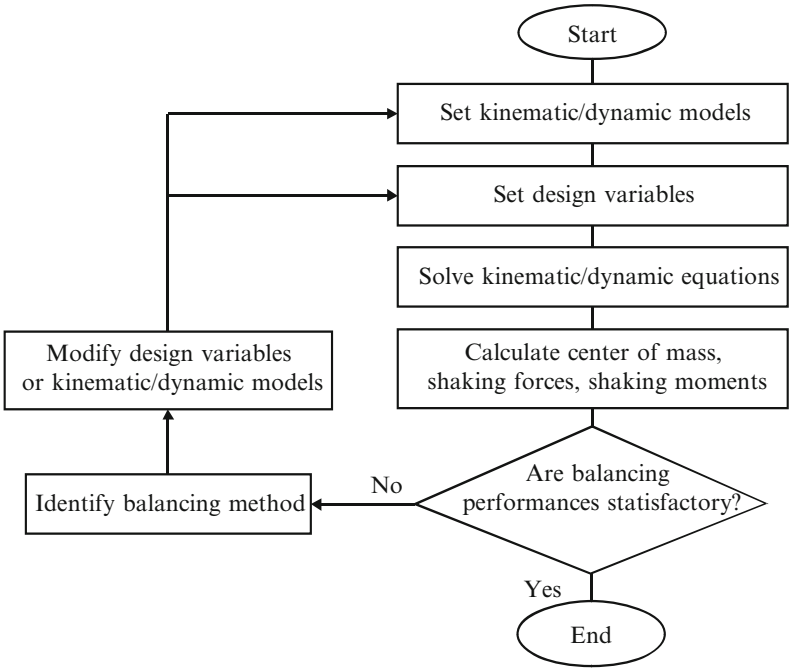

Fig. 8.3 The proposed procedure for balancing

and dynamic models of parallel manipulators is a quite hard task. This topic is widely addressed in the literature as mentioned for example in [36–40]. Close-form solutions of kinematics/dynamics have been identified only for a subset of the feasible kinematic architectures of parallel manipulators. In other cases, simplified and/or approximate and/or iterative approaches should be considered. Then, it is necessary to identify the main characteristics of the system under investigation including masses and inertia properties. The key design variables and sizes should be identified with proper numerical values. Among the design variables special care should be given to the expected input/output motions as function of time.

The solution of kinematics and dynamics equations allows the calculation of the coordinates of center of mass as well as the values of shaking forces and shaking moments. The obtained values depend on the robot architecture but also on the expected input/output motions. Accordingly, coordinates of center of mass as well as the values of shaking forces and shaking moments will be numerically calculated as function of time. The results of these calculations will provide direct information on the fulfilling of static and dynamic balancing conditions.

In general, a mechanism will be statically and dynamically balanced only if—in any operating condition—the calculated coordinates of center of mass coincide with the axis of rotation and the value of shaking forces and shaking moments are zero. However, a designer may desire that a mechanism is just statically balanced or that a mechanism is dynamically balanced only for a specific set of input/output motions. Specific conditions may lead a designer to tolerate a certain amount of unbalancing or even to consider not necessary a static/dynamic balancing. The desired balancing performances should be carefully defined in a case-by-case manner by considering specific design constraints such as construction cost limitations, complexity limitations, size limitations, lightweight requirements, and power consumption improvements.

If the balancing performances are not satisfactory, the procedure will search for a suitable method for fulfilling the desired static/dynamic balancing among those identified in the previous section. Design variables and kinematic/dynamic models should be updated accordingly. Often, it can be necessary to repeat the above procedure in an iterative manner until the desired performances are achieved. A suitable iterative search of proper design variables can be achieved by means of optimal search algorithms while the choice of different balancing methods usually requires a reengineering process.

8.3 A Case of Study for Balancing

A case of study is herewith proposed in order to show the key steps of a balancing design process as referring to a parallel manipulator having three active DOFs.

At LARM in Cassino significant research activity has been devoted to the design of parallel manipulators such as the CaPaMan (Cassino Parallel Manipulator) series. A prototype of CaPaMan 2bis built at LARM is shown in Fig. 8.4. It has been

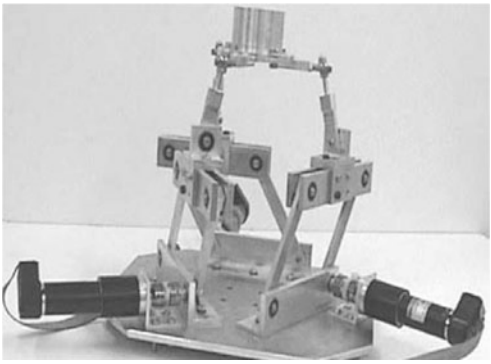

Fig. 8.4 A photo of CaPaMan 2bis

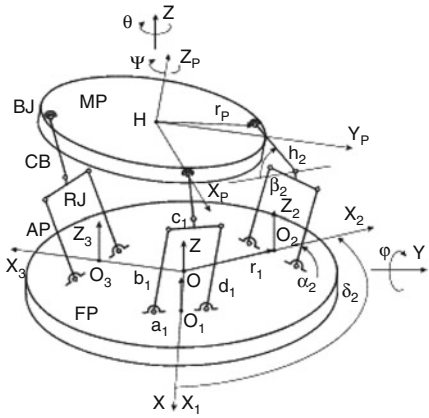

Fig. 8.5 A kinematic scheme of CaPaMan 2bis

implemented as a part of a hybrid robotic architecture for surgical tasks in the work, as well as a trunk module in a humanoid robot design named as CALUMA (CAssino Low-cost hUMAnoid robot) [41–44].

8.3.1 Definition of a Kinematic Model

A kinematic scheme of CaPaMan 2bis is shown in Fig. 8.5. It is composed of a movable platform (MP) connected to a fixed base (FP) through three leg mechanisms. Each leg mechanism is composed of an articulated parallelogram (AP) whose coupler carries a revolute joint (RJ), a connecting bar (CB) that transmits the motion from AP to MP through RJ, and a spherical joint (BJ), which is installed on MP at point J. Revolute joint RJ installed on the coupler of AP has the rotation axis coinciding with the parallelogram plane. Each leg mechanism is rotated $2\pi/3$ with respect to the neighboring one so that the leg planes lie along two vertices of an equilateral triangle, giving symmetry properties to the mechanism. They can be identified for the k-th leg mechanism ($k = 1, 2, 3$) as ak is the length of the frame

link; bk is the length of the input crank; ck is the length of the coupler link; dk is the length of the follower crank; and hk is the length of the connecting bar. The sizes of movable platform MP and fixed base FP are given by distances rp and rf, as shown in Fig. 8.1b. Points H and O are the center points of MP and FP, respectively. Points Ok are the middle point of frame link ak, Jk are the connecting points between. An inertial frame O-XYZ has been assumed to be fixed to base FP. A moving frame HXPYPZP has been attached to platform MP. O-XYZ has been fixed with Z-axis orthogonal to the FP plane and X-axis as coincident with the line joining O to O1. Moving frame HXPYPZP has been fixed to platform MP with ZP orthogonal to the MP plane and XP-axis as coincident to the line joining H to J and YP to give a Cartesian frame. Angle δk is the structure rotation angle between OX1 and OXk as well as between HJ1 and HJk. They are equal to $\delta 1 = 0$, $\delta 2 = 2\pi/3$, and $\delta 3 = 4\pi/3$, the k-th leg mechanism, and platform MP. The design parameters of the CaPaMan 2bis are listed in Table 8.1.

8.3.2 *Definition of a Dynamic Model*

The CaPaMan 2bis parallel manipulator has been modeled using mixed coordinates. So in general terms for a given kinematic chain, the position of each body is described by a set of coordinates that combines reference-point coordinates defined at the center of mass of each body and relative coordinates defined at each joint. In this way a set of dependent coordinates p was defined to describe the manipulator as

$$p = \begin{pmatrix} g_1 \\ e_1 \\ \vdots \\ g_n \\ e_n \end{pmatrix} \tag{8.5}$$

Table 8.1 Mechanical design parameters and inertial properties of CaPaMan 2bis

$a_k = c_k$ (mm)	$b_k = d_k$ (mm)	r_p (mm)	r_f (mm)	h_k (mm)	$I_{cxy} = I_{cxy} = I_{cy}$ (kg mm^2)
100	100	65	65	50	0
α_k (deg)	β_k (deg)	m (kg)	τ (N/m)	I_{czz} (Kg mm^2)	$I_{cxx} = I_{cxy}$ (kg mm^2)
45–135	30–120	2.3	2	24,600	12,400

where g_i are the positions of the center of mass of the body i defined as

$$g_i^{\mathrm{T}} = \left(x_i \; y_i \; z_i\right) \tag{8.6}$$

and e_i are the Euler angles of body i defined in the form

$$\mathrm{e}_i^{\mathrm{T}} = \left(\alpha_i \; \beta_i \; \gamma_i\right) \tag{8.7}$$

In particular for CaPaMan 2bis, 13 bodies were modeled and described by the corresponding set of coordinates, giving a total of 78 coordinates in vector p.

The dynamic equations for parallel architectures are generally difficult to formulate in closed form because of the high nonlinearity existing in the kinematics. A simplification in the dynamic analysis consists of neglecting the inertia of leg mechanisms in comparison with the inertia of the movable plate. This neglecting can be justified when you consider that the leg motion is smoother than that one correspondingly obtained for the movable plate. In fact, the motion and mass of the movable plate are more significant with respect to the corresponding leg properties in most cases. Further details on this matter can be found in [43, 44].

The mobile platform has been transformed in an equivalent model. The equivalence is obtained with three identical point masses arranged symmetrically, shown in Fig. 15, with

$$m_1 = m_2 = m_3 = \tfrac{1}{3}m \tag{8.8}$$

where m is the original total mass of the mobile platform. The only solution to this equivalence is to have

$$y_2 = y_3, \;\; x_2 = -x_3, \;\; y_1 = -2y_2 \tag{8.9}$$

$$I_{xx} = \frac{1}{2}mr_{\mathrm{pm}}, \quad I_{yy} = I_{xx}, \quad I_{zz} = \frac{1}{2}mr_{\mathrm{pm}}, \quad I_{xy} = 0 \tag{8.10}$$

The distance between the center of the mobile platform and the point of attachment to each leg (at the spherical joint) is 65 mm. This means that $r_{\mathrm{pm}} = 65$ mm and using Eq. (8.10), the circular platform results with a diameter of 183.848 mm.

Focusing on the dynamic balancing of CaPaMan 2bis these three point masses are located at the corresponding spherical joints, the points attaching to the legs, so these legs can be balanced independently as shown in Fig. 8.6.

8.3.3 Selection of Design Variables

A 3D CAD model has been built as shown in Fig. 8.7. The model has been simplified so that the mass coming from the equivalence of the moving plate is concentrated at

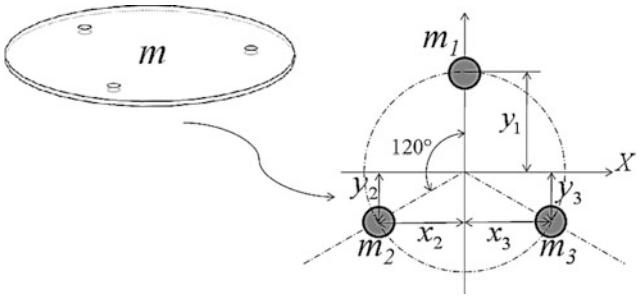

Fig. 8.6 Dynamic equivalence of the mobile platform with three point masses

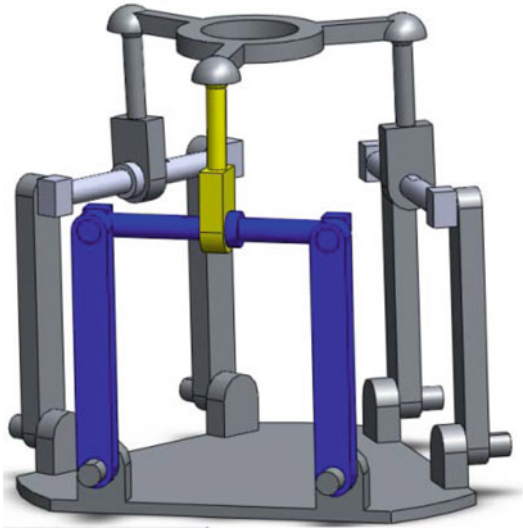

Fig. 8.7 Basic architecture of CaPaMan 2bis indicating the two subsystems that have been used

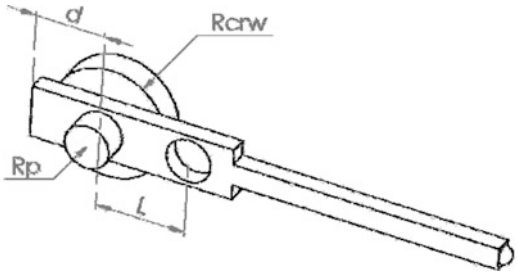

Fig. 8.8 A scheme of a connecting bar CB with main design variables

the spherical joints. Main attention for the balancing will be given to the connecting bars CB (one of them is shown in yellow in Fig. 8.7) and to the coupler-link in the four-bar mechanism (one of them is shown in blue in Fig. 8.7).

The desired balancing condition can be defined so that one can achieve a stationary center of mass. The parameters taken in consideration for the balancing study are shown in Fig. 8.8. The design variables are listed with their properties in Table 8.2.

Table 8.2 The considered feasible ranges of the main design variables

Name	Values	Units
L	Min:10 Max:30	mm
Dp	Min:2 Max:30	mm
d	Min:2 Max:30	mm

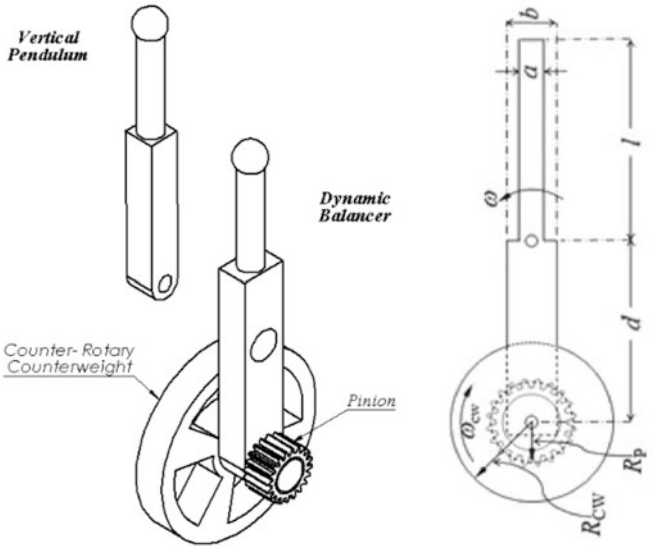

Fig. 8.9 A design for the dynamic balancer: (**a**) Mechanical design layout. (**b**) Design parameters

8.3.4 Choice of Balancing Method

Considering the characteristics of CaPaMan 2bis it can be convenient to select the balancing method that is based on CRCW and counterweights. Given the architecture of CaPaMan 2bis one can use a total of six CRCW and three counterweights.

Once the mobile platform has been split into three point masses, it is possible to balance each leg independently. The original vertical pendulum is modified to become a dynamic balancer. All the geometry of the elements has been simplified, as shown in Fig. 8.9a, in order to facilitate the generation of the balancing equations. The pendulum is a bar with rectangular cross section and thickness $t = 4$ mm. The pinion and CRCW have been considered as solid disks of steel $\left(\rho = 7,800\ {}^{\mathrm{kg}}/_{\mathrm{m}^3}\right)$. The CRCW and the pinion has a thickness of 8.355 mm and are considered of aluminum $\left(\rho = 2,740\ {}^{\mathrm{kg}}/_{\mathrm{m}^3}\right)$. The dynamic balancer is designed in such a way that linear and angular momentum are conserved, getting zero shaking force and zero shaking moment and obtaining a reactionless system.

A constant linear momentum can be obtained if the total center of mass is stationary. Considering **r** as the position vector of the global center of mass one can write

$$\frac{d\mathbf{r}}{dt} = 0 \tag{8.11}$$

that can be expressed as

$$\mathbf{r} = \frac{1}{M}\sum_{i=1}^{n} m_i \mathbf{r}_i; \quad M = \sum_{i=1}^{n} m_i \tag{8.11}$$

where m_i is the mass of the ith body, $\mathbf{r}_i$ is the position vector of the center of mass of the ith body, and M is the total mass of the system.

For the dynamic balancer shown in Fig. 8.9b the global position of the center of mass can be calculated as

$$\mathbf{r} = \frac{1}{M}\left[\frac{1}{3}m_{\mathrm{MP}}l + \frac{1}{2}m_{\mathrm{VP}}l - \frac{1}{2}m_{\mathrm{SB}}d - m_{\mathrm{P}}d - m_{\mathrm{CW}}d\right] \tag{8.12}$$

where $m_{\mathrm{VP}} = \rho_a atl$ is the mass of the vertical pendulum, $m_{\mathrm{SB}} = \rho_a btl$ is the mass of the supporting bar, $m_{\mathrm{P}} = \rho_s \pi t R_{\mathrm{P}}^2$ is the mass of the pinion, and $m_{\mathrm{CW}} = \rho_s \pi t R_{\mathrm{CW}}^2$ is the mass of the CRCW. A point mass of $m_{\mathrm{PM}} = 1.2123$ g, corresponding to one-third of the total mass of the mobile platform, is taken into account.

To impose a stationary center of mass, Eq. (8.12) can be written as

$$\mathbf{r} = \frac{1}{M}\left[1.2123(l) + \frac{1}{2}\mathrm{at}\,(l-d)\,\rho - \frac{1}{2}\pi t d\rho R_P^2 - \frac{3}{2}\pi t d\rho R_{\mathrm{CW}}^2\right] = 0 \tag{8.13}$$

Considering ω as the angular velocity of the bar and ω_{CW} the angular velocity of the pinion-CRCW set, and noting that $\omega_{\mathrm{CW}} = -(d/R_P)\,\omega$, the total angular momentum $\mathbf{H}_{\mathrm{tot}}$ of the system can be calculated as

$$\mathbf{H}_{\mathrm{tot}} = \left[\begin{array}{l} 1.2123\left(l^2\right) + \frac{1}{3}a\rho t\left(l^3 + d^3\right) + \pi\rho t d^2\left(\frac{1}{2}R_P^2 + \frac{3}{2}R_{\mathrm{CW}}^2\right) \\ +\frac{1}{4}\pi\rho t d\left(R_P + 3\frac{R_{\mathrm{CW}}^2}{R_P}\right) \end{array}\right]\omega = 0 \tag{8.14}$$

where the general equation to calculate the moment of inertia of a bar ($I = \frac{1}{12}ml^2$) and the general equation to calculate the moment of inertia of a disk ($I = \frac{1}{2}mR^2$) have been used.

Table 8.3 Results from the solution to get a valid dynamic balancer

l (mm)	a (mm)	b (mm)	t (mm)	T_c (mm)	d (mm)	R_P (mm)	R_{CW} (mm)
64	3	8	4	8.355	40	0.332	7.066

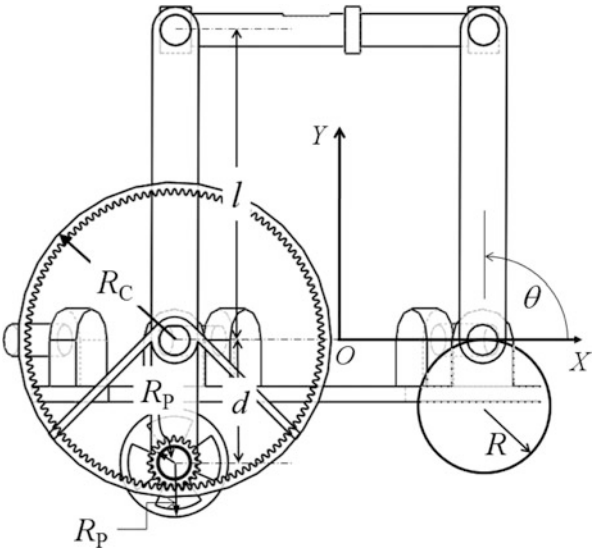

Fig. 8.10 Articulated parallelogram balanced by a single dynamic balancer

Equations (8.13 and 8.14) can be solved simultaneously to obtain a valid dynamic balancer, using an ordinary Newton–Raphson method. The parameters l and a are already determined as they define the pendulum to be balanced, and b has been chosen equal to a (in fact the geometry and dimensions of this part of the dynamic balancer could be a topic to investigate). Different values of d may be chosen, leaving $\mathbf{R_P}$ and as unknowns. Table 8.3 shows representative results choosing $d = 40$ mm, as this value warranties enough distance between the CRCW and the coupler axes of rotation.

The obtained dynamic balancer has been mounted on the coupler of the four-bar linkage (the articulated parallelogram) of the limb, next balanced following a similar procedure as the one used for the vertical pendulum.

The articulated parallelogram can be balanced by a single dynamic balancer and a single counterweight, as in Fig. 8.10, to preserve the linear and angular momentums, obtaining a reactionless system.

The conservation of the linear momentum $\mathbf{L}$ can be obtained by keeping it constant (zero). Linear momentum can be calculated as in Eq. (8.15); two densities are used: ρ_1 is associated to all the elements of the four-bar mechanism, and ρ_2 is associated to the CRCW and to the counterweight. The thickness (t) has been considered the same for all the elements. Additionally take note that a point mass of 0.00121 g is considered, and added to the coupler of the four-bar mechanism.

This point mass comes by considering the basic balancer obtained from the balancing of the vertical pendulum in the form

$$\mathbf{L} = \left\{ \begin{array}{l} \omega \sin(\theta) \left(\begin{array}{l} \pi \rho_2 t R^3 + \pi d \rho_2 t R_P^2 + \pi d \rho_2 t R_{\mathrm{CW}}^2 \\ -2al^2 t \rho_1 - (0.07844) l + \dfrac{1}{2} a d^2 \rho t \end{array} \right) \\ \omega \cos(\theta) \left(\begin{array}{l} -\pi \rho_2 t R^3 - \pi d \rho_2 t R_P^2 - \pi d \rho_2 t R_{\mathrm{CW}}^2 \\ +2al^2 t \rho_1 + (0.07844) l - \dfrac{1}{2} a d^2 \rho t \end{array} \right) \end{array} \right\} = \text{const.} \tag{8.15}$$

Constant linear momentum can be achieved if the sum of terms in the parenthesis of Eq. 8.15 is zero; this is the necessary condition to get null shaking force. Therefore, one can write

$$\begin{aligned} &\pi \rho_2 t R^3 + \pi d \rho_2 t R_P^2 + \pi d \rho_2 t R_{\mathrm{CW}}^2 \\ &\quad - 2al^2 t \rho_1 - (0.07844) l + \frac{1}{2} \mathrm{ad}^2 \rho t = 0 \end{aligned} \tag{8.16}$$

On the other hand to get a null shaking moment it is necessary to make the total angular momentum of the system constant or zero. For the articulated parallelogram shown in Fig. 20 the total angular momentum can be calculated as

$$\begin{aligned} H_Z = \omega &\left(\begin{array}{l} \dfrac{3}{2} \pi \rho_2 t R^4 - \dfrac{1}{2} \pi d \rho_2 t R_P^3 + \pi d^2 \rho_2 t R_P^2 - \dfrac{1}{2} \dfrac{\pi d \rho_2 t R_{\mathrm{CW}}^4}{R_P} \\ + \pi d^2 \rho_2 t R_{CW}^2 + \dfrac{5}{3} a l^3 t \rho_1 + \dfrac{1}{3} \mathrm{ad}^3 t \rho_1 + (0.07844) l^2 \end{array} \right) \\ + \omega \cos(\theta) &\left(\begin{array}{l} \dfrac{1}{2} \pi l \rho_2 t R^3 - \dfrac{1}{2} \pi d l \rho_2 t R_P^2 \\ -\dfrac{1}{2} \pi d l \rho_2 t R_{CW}^2 - \dfrac{1}{4} d^2 l t \rho_1 \end{array} \right) = 0 \end{aligned} \tag{8.17}$$

ω is the angular velocity of both cranks (the coupler never rotates); it has also been considered that $\omega_{\mathrm{CW}} = -(d/R_P)\,\omega$ is the angular velocity of the CRCW-pinion set, just as in the vertical pendulum case. To get a constant angular momentum both terms in parenthesis in Eq. (8.17) must be zero, and then the conditions to accomplish can be summarized as

$$\begin{aligned} &\frac{3}{2} \pi \rho_2 t R^4 - \frac{1}{2} \pi d \rho_2 t R_P^3 + \pi d^2 \rho_2 t R_P^2 - \frac{1}{2} \frac{\pi d \rho_2 t R_{\mathrm{CW}}^4}{R_P} \\ &\quad + \pi d^2 \rho_2 t R_{\mathrm{CW}}^2 + \frac{5}{3} a l^3 t \rho_1 + \frac{1}{3} a d^3 t \rho_1 + (0.07844) l^2 = 0 \end{aligned} \tag{8.18}$$

$$\frac{1}{2} \pi l \rho_2 t R^3 - \frac{1}{2} \pi d l \rho_2 t R_P^2 - \frac{1}{2} \pi d l \rho_2 t R_{\mathrm{CW}}^2 - \frac{1}{4} d^2 l t \rho_1 = 0 \tag{8.19}$$

Table 8.4 Balancing results

l (mm)	a (mm)	t (mm)	R_P (mm)	d (mm)	R (mm)	R_{CW} (mm)
70	5	10	5	2.5	17.2	44.2

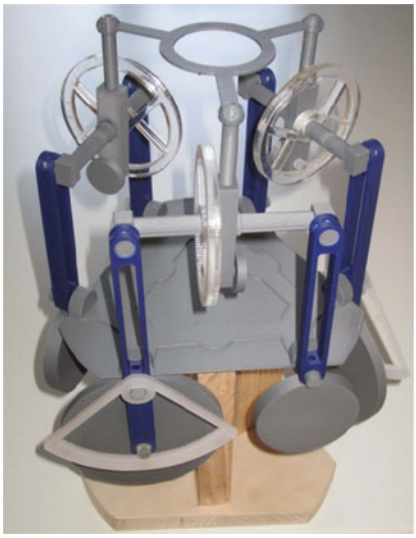

Fig. 8.11 Modified CaPaMan 2bis concept with counter-rotary counterweights and counterweights [28]

The latter can be solved simultaneously using the Newton–Raphson algorithm for a set of nonlinear equations. In this case the length (l) of both cranks and the coupler (considered made of aluminum with $\rho_1 = 2740\ {}^{\text{kg}}/_{\text{m}^3}$) of the articulated parallelogram is known, $l = 70$ mm, and the width and the thickness are set to $a = 10$ mm and $t = 10$ mm, respectively, for all elements. The CRCW and the counterweight are considered made of steel, with $\rho_2 = 7,800\ {}^{\text{kg}}/_{\text{m}^3}$. Finally the radius of the pinion is set to $R_P = 5$ mm, even though it is possible to choose any other value, taking into account that the lesser value the bigger the radius of the CRCW. Solutions are shown in Table 8.4. The final design with the modified parts is shown in Fig. 8.11.

8.3.5 Numerical Validation of Balancing

The balancing computation verified has been with a dynamic simulation using MSC ADAMS imposing some general motions to the DOFs associated to the cranks in the articulated parallelograms. Three generic cubic functions have been used to guide the 3-DOFs in the form

$$\alpha_i = \alpha_{i0} + \frac{3\Delta\alpha_i}{t_{\text{if}}^2} t^2 - \frac{2\Delta\alpha_i}{t_{\text{if}}^3} t^3; \quad \Delta\alpha_i = \alpha_{\text{if}} - \alpha_{i0} \tag{8.20}$$

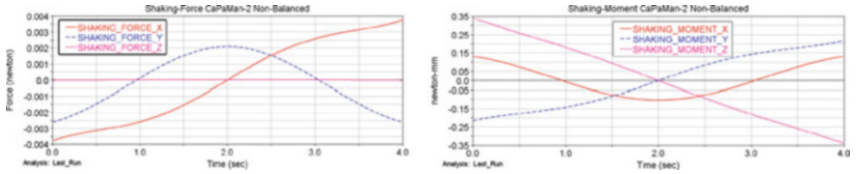

Fig. 8.12 Computed results from the simulation of the ADAMS non-balanced model: (**a**) Shaking forces, (**b**) shaking moments

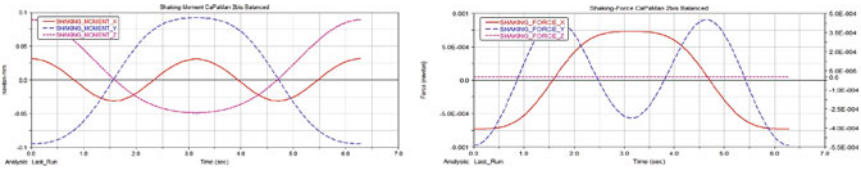

Fig. 8.13 Computed results from the simulation of the ADAMS balanced model: (**a**) Shaking forces, (**b**) shaking moments

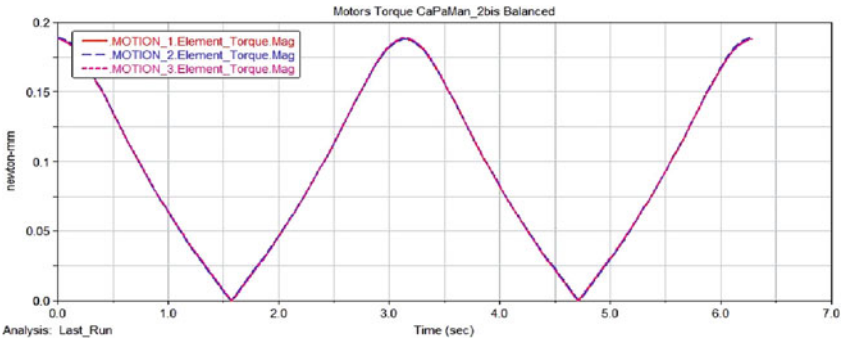

Fig. 8.14 Needed motor torque

Applying the function in Eq. 39 to one leg and keeping the other ones fixed the results obtained in the non-balanced mechanism are presented in Fig. 8.12, while the results obtained in the balanced mechanism are presented in Fig. 8.13. With the balancing procedure shaking forces in X and Y drop by an order of magnitude and shaking forces in Z remain constantly zero. A significant improvement is noticed in the shaking moments especially in Y and Z, the most important axis concerning vibrations due to the nature of the model motion. Analyzing the motor torques shown in Fig. 8.14 it can be noticed that also if more mass has been added the needed torque to move the manipulator is very low.

The application of CRCW to the dynamic balancing of a spatial 3-DOFs parallel manipulator, given the special architecture of the mechanism, shows that this procedure leads to very good results in shaking force and to an interesting reduction in shaking moment.

8.4 Conclusions

This chapter has addressed the key issues for achieving static and dynamic balancing of a robotic system. A general procedure has been outlined in order to clarify the main steps that should be considered in the design process for achieving suitable balancing performances. The proposed procedure has been considered specifically for manipulators having parallel architecture. A case of study has been reported in full details in order to show the feasibility and effectiveness of the proposed procedure. In particular, the proposed case of study refers to a 3-DOFs parallel manipulator, whose name is CaPaMan 2bis. The main result of the proposed balancing procedure has been the improvement of CaPaMan 2bis design for dynamically balanced operation. A numerical simulation has been carried out in MSC.ADAMS environment for validating the expected dynamic performances of the improved CaPaMan 2bis design.

Acknowledgements Authors wish to acknowledge the significant contribution and inspiration to this chapter given by Prof. Mario Acevedo, Universidad Panamericana, Mexico City.

References

1. Uicker, J.J., Pennock, G.R., Shigley, J.E.: Theory of machines and mechanisms. Oxford University Press, New York (2003)
2. Angeles, J.: Dynamic response of linear mechanical systems, modeling, analysis and simulation. Springer, (2012)
3. Norton, M.P., Karczub D.G.: Fundamentals of noise and vibration analysis for engineers. Cambridge University Press, (2003)
4. International Organization for Standardization (ISO): Mechanical vibration—Balancing—Guidance on the use and application of balancing standards. ISO 19499, (2007)
5. International Organization for Standardization (ISO): Test methods for measuring tyre uniformity. ISO 13326, (1998)
6. Ceccarelli, M.: Fundamentals of mechanics of robotic manipulation. Kluwer Academic Publishers, (2004)
7. Arakelian, V.H., Briot, S.: Dynamic balancing of the Scara robot. Proceedings of the 17-th CISM-IFToMM Symposium on Robot Design, Dynamics and Control (RoManSy 2008), Tokyo, pp. 167–174 (2008)
8. Rivin, E.I.: Mechanical design of robots. McGraw Hill, (1987)
9. Kemmerling, P.T Jr.: Dynamic characteristics of flight simulator motion systems. Agard Conference Proceedings No. 249, London, p. 20, 1978, available on-line at http://www.dtic.mil/dtic/tr/fulltext/u2/a063850.pdf
10. Agrawal, A., Agrawal, S.K.: Design of gravity balancing leg orthosis using non-zero free length springs. Mech. Mach. Theory **40**, 693–709 (2005)
11. Xu, Y., Au, K.W., Nandy, G.C., Brown H.B.: Analysis of actuation and dynamic balancing for a single-wheel robot. IEEE/RSJ International Conference on Intelligent Robots and Systems. Vol. 3 pp. 1789–1794, Victoria, (1998)
12. Park, J., Haan, J., Park, F.C.: Convex optimization algorithms for active balancing of humanoid robots. IEEE Trans. Robot. **23**(4), 817–822 (2007)

13. Berkof, R.S., Lowen, G.G.: A new method for completely force balancing simple linkages". J. Eng. Ind. **91**(B), 21–26 (1969)
14. Arakelian, V.H., Smith, M.R.: Complete shaking force and shaking moment balancing of linkages. Mech. Mach. Theory **34**(8), 1141–1153 (1999)
15. Arakelian, V.H., Smith, M.R.: Shaking force and shaking moment balancing of mechanisms: a historical review with new examples. ASME Trans. J. Mech. Des. **127**, 334–339 (2005)
16. Kochev, I.S.: General theory of complete shaking moment balancing of planar linkages: a critical review". Mech. Mach. Theory **35**, 1501–1514 (2000)
17. Herder J.L., Gosselin C.M.: A Counter-Rotary Counterweight (CRCW) for Light-Weight Dynamic Balancing. Proceedings of the ASME Design Engineering Technical Conferences and Computers and Information in Engineering Conference, Salt Lake City, Utah, USA, September 28-October 2, (2004)
18. Russo, A., Sinatra, R., Xi, F.: Static balancing of parallel robots". Mech. Mach. Theory **40**, 191–202 (2005)
19. Van der Wijk V., Herder, J.: Synthesis of dynamically balanced mechanisms by using counter-rotary countermass balanced double pendula. ASME J. Mech. Des., **131**(11), (2009)
20. Van der Wijk, V.L., Herder, J., Demeulenaere, B.: Comparison of various dynamic balancing principles regarding additional mass and additional inertia. J. Mech. Robot., JMR-08-1193, (2009)
21. Wu, Y., Gosselin, C.M.: On the Dynamic Balancing of Multi-DOF Parallel Mechanisms With Multiple Legs". ASME J. Mech. Des. **129**(2), 234–238 (2007)
22. Lim, T.G., Cho, H.S., Chung, W.K.: A parameter identification method for robot dynamic models using a balancing mechanism. Robotica Int. J. **7**(4), 327–337 (1989)
23. Rahman, T., Ramanathan, R.: A simple technique to passively gravity-balance articulated mechanisms. ASME J. Mech. Des. **117**(4), 655–658 (1995)
24. Deepak S.R., Ananthasuresh G.K.: Static balancing of a four-bar linkage and its cognates. Mech. Mach. Theory. (2011)
25. Ebert-Uphoff, I., Gosselin, C.M., Laliberté, T.: Static balancing of spatial parallel platform mechanisms-revisited". J. Mech. Des. **122**, 43–51 (2000)
26. Elliot J.L., Tesar D.: The theory of torque, shaking force and shaking moment balancing of four link mechanisms. ASME J. Eng. Ind. **99**, (1977)
27. Gosselin, C.M., Vollmer, F., Côté, G., Wu, Y.: Synthesis and design of reactionless three-degree-freedom parallel mechanisms. IEEE Trans Robot. Automat. **20**(2), (2004)
28. Acevedo, M., Ceccarelli, M., Carbone, G., Cafolla, D.: Complete dynamic balancing of a 3-DOFs spatial parallel mechanisms by the application of counter-rotary counterweights. EUROMECH Colloquium 524, University of Twente, Enschede, Netherlands, February 27 March 1, (2012)
29. Gosselin, C.M., Vollmer, F., Côté, G., Wu, Y.: Synthesis and Design of Reactionless Three-Degree-of-Freedom Parallel Mechanisms". IEEE Trans. Robot. Automat. **20**(2), 191–199 (2004)
30. Gosselin, C.M., Moore, B., Schicho, J.: Dynamic balancing of planar mechanisms using toric geometry. J. Symbolic Comput. In Press, Accepted Manuscript (2009)
31. Laliberté, T., Gosselin, C.M., Jean, M.: Static balancing of 3-DOFs planar parallel mechanisms. IEEE/ASME Trans. Mechatron. **4**, 363–377 (1999)
32. Moore, B., Schicho, J., Gosselin, C.M.: Dynamic balancing of spherical 4r linkages. J. Mech. Robot. Submitted, paper number JMR-08-1176, (2009)
33. Xi, F.: Dynamic balancing of hexapods for high-speed applications. Robotica Int. J. **17**(3), 335–342 (1999)
34. Alici, G., Shirinzadeh, B.: Optimum synthesis of planar parallel manipulators based on kinematic isotropy and force balancing. Robotica Int. J. **22**(1), 97–108 (2004)
35. Alici, G., Shirinzadeh, B.: Optimum dynamic balancing of planar parallel manipulators based on sensitivity analysis. Mech. Mach. Theory **41**(12), 1520–1532 (2006)
36. Angeles, J.: Fundamentals of robotic mechanical systems: theory, methods, and algorithms. Springer, Dordrecht (2006)

37. Ceccarelli, M.: Fundamentals of mechanics of robotic manipulation. Kluwer Academic Publisher, Dordrecht (2004)
38. Merlet, J.P.: Parallel robots. Springer, Dordrecht (2006)
39. García de Jalón, J., Bayo, E.: Kinematic and dynamic simulation of multibody systems: the real-time challenge. Springer, New York (1994)
40. Rolland, L.: Certified solving of the forward kinematics problem with an exact method for the general parallel manipulators. Int. J. Robot. Soc. Japan **19**(9), 995–1025 (2005)
41. Aguirre, G., Acevedo, M., Carbone, G., Ceccarelli, M.: Kinematic and dynamic analyses of a 3-DOFs parallel manipulator by symbolic formulations. Thematic Conference on Advances in Computational Multibody Dynamics, ECCOMAS Lisbon, Paper MB2003-010, (2003)
42. Hernandez-Martinez, E.E., Conghui, L., Carbone, G., Ceccarelli, M., Lopez-Cajun, C.S.: Experimental and Numerical Characterization of CaPaMan 2bis Operation". J. Appl. Res. Technol. **8**(1), 101–119 (2010)
43. Carbone, G., Ceccarelli, M., Oliveira, P.J., Saramago, S.F.P., Carvalho, J.C.M.: Optimum Path Planning of CaPaMan (Cassino Parallel Manipulator) by Using Inverse Dynamics". Robotica: Int. J. **26**(2), 229–239 (2008)
44. Carvalho, J.C.M., Ceccarelli, M.: A closed form formulation for the inverse dynamics of cassino parallel manipulator. J. Multibody Syst. Dynamics **5**, 185–210 (2001). Vol. 6, pp.303